# A Co-optimization Model for the Restoration of Wildfire-damaged Electrical Distribution Systems

Brent Austgen, Ross Guttromson
*Electric Power Systems Research Department*
*Sandia National Laboratories*
Albuquerque, New Mexico, USA
{bgaustg,rguttro}@sandia.gov

***Abstract*—The restoration of electrical distribution systems following wildfire damage is often approached using a combination of established procedures and improvised planning. This paper introduces a multi-period co-optimization model designed for use in a rolling-horizon approach to decision making for restoration of fire-damaged electrical utility infrastructure. By leveraging real-time data collected from utilities, wildfire response teams, and emergency organizations, our model provides a structured approach to decision making over the course of a wildfire restoration. The model's primary objective is to maximize criticality-weighted load served. The model accounts for critical factors such as power grid operations, topology adjustments, and utility crew scheduling while adhering to practical constraints, including travel and repair times, resource availability, and crew safety. Uncertainty of future wildfire conditions is incorporated in the form of a multi-period forecast. Ultimately, the model prescribes actionable recommendations that enable utilities to make informed decisions about resource allocation and job scheduling during wildfire events.**

***Index Terms*—forecast, multi-period, optimization, power grid, restoration, rolling horizon, wildfire**

## NOMENCLATURE

### Sets

| | |
|---|---|
| $\mathcal{T}$ | time periods |
| $\mathcal{N}$, $\mathcal{N}_n$ | power grid sections, sections neighboring section $n$ |
| $\mathcal{L}$ | directed power grid switches, $\mathcal{L} \subseteq \mathcal{N} \times \mathcal{N}$ |
| $\mathcal{O}$, $\mathcal{O}_{nm}$ | switch configurations, configurations in which switch $(n, m)$ may be closed |
| $\mathcal{S}$, $\mathcal{S}_s$ | sites, sites with travel option to/from site $s$ |
| $\mathcal{Q}$ | site-to-site travel options ($\mathcal{Q} \subset \mathcal{S} \times \mathcal{S}$) |
| $\mathcal{J}$, $\mathcal{J}_s$, $\mathcal{J}_n$ | jobs, jobs at site $s$, jobs in section $n$ |
| $\mathcal{C}$, $\mathcal{C}_j$ | capabilities, capabilities required by job $j$ |
| $\mathcal{R}$, $\mathcal{R}_c$ | resource types, types that provide capability $c$ |

### Parameters

| | |
|---|---|
| $a_r$ | number of available type-$r$ resources |
| $t_n^{\text{dmg}}$ | time period that damage first occurs in section $n$ |
| $t_j^{\text{job}}$ | earliest time period that job $j$ may begin |
| $d_j^{\text{job}}$ | time periods required to complete job $j$ |
| $d_{s,s'}^{\text{travel}}$ | time periods required to travel from site $s$ to $s'$ |
| $g_{cj}$ | number of resources with capability $c$ needed for job $j$ |
| $\alpha_{st}$ | indicator that it is unsafe to be idle or working at site $s$ in time period $t$ |
| $\beta_{ss't}$ | indicator that it is unsafe to begin travel from site $s$ to site $s'$ at time $t$ |
| $\rho_n$ | criticality of load in section $n$ |
| $p_{nt}^{\text{load}}$ | load in section $n$ at time $t$, |
| $p_n^{\text{supply}}$ | power supply capacity of section $n$ |
| $p_{nm}^{\text{flow}}$ | maximum power flow across branch $(n, m)$ |
| $\delta$ | time discounting factor |

### Variables

| | |
|---|---|
| $\hat{p}_{nt}$ | power sourced in section $n$ at time $t$ |
| $\check{p}_{nt}$ | power served in section $n$ at time $t$ |
| $\tilde{p}_{nmt}$ | power flow from section $n$ to $m$ at time $t$ |
| $u_{ot}$ | indicator that configuration $o$ is active at time $t$ |
| $v_{nmt}$ | indicator that switch $(n, m)$ is closed at time $t$ |
| $\underline{w}_{jt}$ | indicator that job $j$ starts at time $t$ |
| $\overline{w}_{jt}$ | indicator that job $j$ is done by time $t$ |
| $x_{rst}$ | # type-$r$ resources present at site $s$ at time $t$ |
| $\hat{x}_{rst}$ | # type-$r$ resources disabled at site $s$ at time $t$ |
| $w_{rjct}$ | # type-$r$ resources using capability $c$ on job $j$ at time $t$ |
| $w'_{rjct}$ | # type-$r$ resources using capability $c$ on job $j$ beginning at time $t$ |
| $y_{rss't}$ | # type-$r$ resources departing for site $s'$ from $s$ at time $t$ |
| $z_{rst}$ | # type-$r$ resources joining from site $s$ at time $t$ |

Sandia National Laboratories is a multimission laboratory managed and operated by National Technology & Engineering Solutions of Sandia, LLC, a wholly owned subsidiary of Honeywell International Inc., for the U.S. Department of Energy's National Nuclear Security Administration under contract DE-NA0003525. SAND2026-17163C.

## I. INTRODUCTION

The restoration of electrical distribution systems following wildfire damage is often approached using a combination of established procedures and improvised planning [1]. Traditional approaches to determining an optimal restoration order may seem straightforward when considering the grid in isolation; however, such approaches overlook critical factors such as utility resources, transportation network damage, and wildfire uncertainty. These complexities can significantly impact decision making processes, leading to inefficiencies and prolonged outages for customers.

Holistic approaches to power system restoration planning are well-documented in the research literature. For instance, in [2], the authors propose a one-shot model for planning transmission system restoration that integrates grid operations with the scheduling of individual component repairs. Similarly, the rolling-horizon approach to distribution system restoration presented in [3] addresses the coordination of damage

979-8-3315-8138-1

assessment, fault isolation, crew routing, repair, and load re-energization. However, these models focus on decision making strictly after the system has sustained all damage, which may not adequately address the complexities of wildfires that can cover wide geographical areas and persist for weeks or even months. In such scenarios, restoration strategies must account for reactive measures to address already-realized impacts and proactive measures to prepare for anticipated future impacts. This dual challenge underscores the need for a more structured approach to restoration that can adapt to the dynamic nature of wildfire events.

In this paper, we introduce a co-optimization model for informing distribution grid restoration decisions during and after a wildfire. Like many existing approaches, our proposed model integrates multiple interconnected decision domains. Specifically, we integrate grid operation, job scheduling, and resource dispatching. What sets our model apart is that it meets the aforementioned dual challenge by accounting for already-realized wildfire impacts as well as forecasted future impacts. The model is intended for use in a rolling-horizon approach that leverages real-time data streams, including forecast data, to continually inform near-term restoration activities while simultaneously mitigating the risk of uncertain future conditions. With this approach, our goal is to formalize operational decision support for utilities by dynamically providing actionable recommendations and insights that account for the complexities of wildfire restoration, particularly those that necessitate strategies with both reactive and proactive components.

The proposed model features a simplified graph representation of the distribution grid, where nodes represent isolable radial sections and edges represent switches. Switching actions are restricted by a set of predetermined vetted topology configurations that ensure safe and stable operation of the distribution grid. Resource dispatching decisions are governed by temporal constraints that account for resource staging, travel times on a potentially damaged road network, job completion times, and resource safety. Resource dispatching and job scheduling decisions are linked by constraints that assign resource capabilities to job requirements. Job scheduling and grid operation decisions are linked by the completion of repair jobs in each grid section. The model's objective function seeks to co-optimize criticality-weighted customer load served (maximize), the number of completed jobs (maximize), and the number of resources exposed to dangerous wildfire conditions (minimize). The model solution prescribes how utility resources should be used to complete jobs that facilitate the re-energization of customer loads.

In the following sections, we formulate and describe the proposed co-optimization model, present a case study that exercises the model in the context of a wildfire threat, analyze the model solution for the case study, and finally discuss our findings and the potential for future research in this domain.

## II. Model Formulation

Our proposed model links three decision domains: distribution grid operation, job scheduling, and resource dispatching. Time-indexed parameters comprise a forecast, and time-indexed variables represent a coordinated response to that forecast. The objective function is

$$\sum_{t\in\mathcal{T}}\delta^t\bigg(\lambda^{\text{load}}\sum_{n\in\mathcal{N}}\rho_n\check{p}_{nt}+\lambda^{\text{job}}\sum_{j\in\mathcal{J}}\overline{w}_{jt}-\lambda^{\text{res}}\sum_{\substack{r\in\mathcal{R}\\ s\in\mathcal{S}}}\hat{x}_{rst}\bigg), \quad (1)$$

which we seek to maximize. Each domain contributes one metric to (1). For grid operation, the aim is to maximize the criticality-weighted load served. Re-energizing a load typically requires completing multiple jobs. The job scheduling objective focuses on maximizing the number of completed jobs, even those that do not directly facilitate load re-energization within the finite time horizon. The resource dispatching goal is to minimize the number of resources rendered inoperative due to hazardous conditions. We would prefer to prohibit inoperative resources, but doing so in a rolling-horizon approach with forecast error can lead to model infeasibility. For $\delta\in(0,1)$, $\delta^t$ decays in $t$, thus prioritizing imminent decisions that affect benefits and costs between the current and next epochs in the rolling-horizon approach. The weights $\lambda^{\text{load}}$, $\lambda^{\text{job}}$, and $\lambda^{\text{res}}$, which govern the relative priorities of the metrics, reflect decision maker preferences.

Our model of distribution grid operation is governed by the following constraints:

$$\hat{p}_{nt}-\check{p}_{nt}=\sum_{m\in\mathcal{N}_n}\left(\tilde{p}_{nmt}-\tilde{p}_{mnt}\right), \quad \forall n\in\mathcal{N}, t\in\mathcal{T}, \quad (2)$$

$$\tilde{p}_{nmt}\le p^{\text{flow}}_{nm}v_{nmt}, \quad \forall(n,m)\in\mathcal{L}, t\in\mathcal{T}, \quad (3)$$

$$\sum_{o\in\mathcal{O}}u_{ot}=1, \quad \forall t\in\mathcal{T}, \quad (4)$$

$$v_{nmt}\le\sum_{o\in\mathcal{O}_{nm}}u_{ot}, \quad \forall(n,m)\in\mathcal{L}, t\in\mathcal{T}. \quad (5)$$

We model the distribution grid as a graph, where isolable sections are represented as nodes and the switches connecting them as edges. Sections may function as power sources (e.g., substations), power sinks (e.g., customer loads), or both. Constraints (2) ensure power flow balance, while constraints (3) prevent power flow across open switches. Topological restrictions (e.g., radiality) are enforced through switch configurations, defined as a partition of switches into those that may be closed and those that must remain open. Constraints (4) ensure that exactly one configuration is active at any time, and constraints (5) prevent a switch from being closed unless permitted by the active configuration. To ensure robust grid operation via constraints (4) and (5), the set $\mathcal{O}$ must be carefully parametrized. Advanced modeling tools capable of evaluating tie line closures, voltage stability, protection adequacy, etc. should be used to that end. Grid operation variables are bounded independently as follows: $\hat{p}_{nt}\in[0,p^{\text{supply}}_{nt}]$, $\check{p}_{nt}\in[0,p^{\text{load}}_{nt}]$, $\tilde{p}_{nmt}\in[0,p^{\text{flow}}_{nm}]$, $u_{ot}\in\{0,1\}$, and $v_{nmt}\in\{0,1\}$.

Switch closures are further constrained by the state of the restoration process:

$$v_{nmt}\le\overline{w}_{jt}, \quad \forall(n,m)\in\mathcal{L}, \forall j\in\mathcal{J}_m, \forall t\in\mathcal{T}: t\ge t^{\text{dmg}}_m. \quad (6)$$

Constraints (6) ensure that a switch cannot be closed unless both sections adjacent to the switch are restored (i.e., all

979-8-3315-8138-1

jobs in the section are completed), thereby preventing an energized section from connecting to a faulted section. This linkage between distribution grid operation and job scheduling is crucial.

The core job scheduling constraints are

$$\sum_{t\in\mathcal{T}} \underline{w}_{jt} \le 1, \qquad \forall j \in \mathcal{J}, \tag{7}$$

$$\underline{w}_{jt} = 0, \qquad \forall j \in \mathcal{J}, \forall t \in \mathcal{T}\colon t < t_j^{\text{job}}, \tag{8}$$

$$\overline{w}_{jt} \le \overline{w}_{j,t-1} + \underline{w}_{j,t-d_j^{\text{job}}}, \quad \forall j \in \mathcal{J}, \forall t \in \mathcal{T}\colon t > d_j^{\text{job}}, \tag{9}$$

$$\overline{w}_{jt} \ge \underline{w}_{j,t-d_j^{\text{job}}}, \qquad \forall j \in \mathcal{J}, \forall t \in \mathcal{T}\colon t > d_j^{\text{job}}, \tag{10}$$

$$\overline{w}_{jt} \ge \overline{w}_{j,t-1}, \qquad \forall j \in \mathcal{J}, \forall t \in \mathcal{T}\colon t > 1. \tag{11}$$

To model job scheduling, we utilize two sets of decision variables: $\underline{w}_{jt} \in \{0,1\}$ to indicate the start of job $j$ in time period $t$ and $\overline{w}_{jt} \in \{0,1\}$ to indicate its completion by time period $t$. Constraints (7) ensure each job starts at most once, and constraints (8) prevent premature job initiation. Constraints (9)–(11) ensure that a job is completed by time $t$ if and only if it was started at $t - d_j^{\text{job}}$ or completed by $t-1$.

Each job requires specific types of resources to initiate:

$$g_{cj}\underline{w}_{jt} = \sum_{r\in\mathcal{R}_c} w'_{rjct}, \quad \forall j \in \mathcal{J}, \forall c \in \mathcal{C}_j, \forall t \in \mathcal{T}. \tag{12}$$

Constraints (12) link the job scheduling and resource dispatching domains. To model resource dispatching, we differentiate between when a resource works on a job and when it *starts* work. The relationship is expressed as

$$w_{rjct} = \sum_{t'=\max\{t-d_j^{\text{job}}+1,1\}}^{t} w'_{rjct'}, \quad \forall r\in\mathcal{R}, j\in\mathcal{J}, c\in\mathcal{C}_j, t\in\mathcal{T}. \tag{13}$$

Constraints (13) ensure that the number of resources working on a job at time $t$ equals those that started working on that job in the last $d_j^{\text{job}}$ time periods (including period $t$), ensuring continuous work on a job once initiated.

The core resource dispatching constraints are

$$x_{r,s,t} = \mathbb{I}_{[t>1]}x_{r,s,t-1} + z_{r,s,t} + \sum_{s'\in\mathcal{S}_s}\Big(\mathbb{I}_{[t-d^{\text{travel}}_{s',s}>1]}y_{r,s',s,t-d^{\text{travel}}_{s',s}} - y_{r,s',s,t}\Big), \quad \forall r\in\mathcal{R}, s\in\mathcal{S}, t\in\mathcal{T}, \tag{14}$$

$$\hat{x}_{r,s,t} = \mathbb{I}_{[t>1]}(1-\alpha_{s,t})\hat{x}_{r,s,t-1} + \alpha_{s,t}x_{r,s,t}, \quad \forall r\in\mathcal{R}, s\in\mathcal{S}, t\in\mathcal{T}, \tag{15}$$

$$x_{r,s,t} \ge \sum_{\substack{j\in\mathcal{J}_s\\ c\in\mathcal{C}_j\cup\mathcal{C}_r}} w_{r,j,c,t} + \hat{x}_{r,s,t}, \qquad \forall r\in\mathcal{R}, s\in\mathcal{S}, t\in\mathcal{T}. \tag{16}$$

For each resource type $r$ and site $s$, constraints (14) ensure that the number of resources present at time $t$ equals the number present at time $t-1$, plus any resources that join or arrive at time $t$, minus those that leave at time $t$. Similarly, constraints (15) dictate that the number of disabled resources at time $t$ is a function of site safety. When a site is safe ($\alpha_{st} = 0$), then the number of disabled resources is the same as in the previous time period. When it is unsafe ($\alpha_{st} = 1$), then all present resources are disabled. Constraints (16) ensure that the number of resources working at a site does not exceed the number of resources present, minus those that are disabled. Disabled resources represent those that permanently cease restoration activities following dangerous contact with the wildfire. Crucially, constraints (15) and (16) together ensure disabled resources neither move from nor work at the site at which they are disabled.

Other constraints regarding resource safety include

$$w_{rjct} \le M(1-\alpha_{st}), \forall r\in\mathcal{R}, s\in\mathcal{S}, j\in\mathcal{J}_s, c\in\mathcal{C}_r\cup\mathcal{C}_j, t\in\mathcal{T}, \tag{17}$$

$$y_{rss't} \le M(1-\beta_{ss't}), \ \forall r\in\mathcal{R}, (s,s')\in\mathcal{Q}, t\in\mathcal{T}. \tag{18}$$

Constraints (17) and (18), respectively, prevent resources from working at unsafe sites and from moving between sites that have no safe site-to-site travel option. We formulate these constraints here using the big-$M$ method, but these constraints can be efficiently implemented by conditionally fixing variables (e.g., $\beta_{ss't} = 1 \implies y_{rss't} = 0, \forall r \in \mathcal{R}$).

Resources joining the restoration effort are restricted via

$$\sum_{\substack{s\in\mathcal{S}\\ t\in\mathcal{T}}} z_{rst} \le a_r, \quad \forall r \in \mathcal{R}. \tag{19}$$

Constraints (19) ensure that no more resources of a given type join the restoration than are available. Additional conditions, such as requiring resources to join from designated staging sites, may be incorporated as needed.

Finally, the resource dispatching variables in constraints (13)-(19) are restricted to the non-negative integers.

## III. Case Study

We now introduce a case study that incorporates a realistic feeder, real geography, a simulated wildfire event, and a fictitious utility company. In building the case study, we balance adding detail to exercise the optimization model with maintaining simplicity to validate the model using our intuition. This section is organized into three subsections: distribution feeder, road network, and utility response to wildfire impact. Throughout these subsections, we reference Fig. 1 for a spatial depiction of the case study and Table I for model parameters that differ by feeder section. The first column indicates the section, and the second column indicates the load in each section, which we suppose remains constant in time. The remaining columns describe parameters that characterize the wildfire's impact. For this off-line analysis, we estimated these parameters using FlamMap [4], a wildfire simulation tool that accounts for ground topology, fuel, and wind, and declaring damage where the simulated wildfire coincides with the distribution infrastructure per Fig 1. In operational use, this information would come from utility estimators, wildfire forecasters, or other agencies.

Some sets and parameters do not fit the aforementioned categories. We define $\mathcal{T} = \{1,\ldots,96\}$ with each time period representing one hour. In (1), we select a mild time-discounting factor of $\delta = 0.99$. Depending on the frequency of epochs in the rolling-horizon approach, which we do not demonstrate in this case study, this parameter could be selected

979-8-3315-8138-1

TABLE I
CASE STUDY PARAMETERS BY GRID SECTION

| Section $n$ | $p^{\text{load}}_{nt}$ (kW) | $t^{\text{dmg}}_n$ | $t^{\text{job}}_j$ | Transformer Jobs | Conductor Jobs |
|---|---|---|---|---|---|
| 0 | 0 | - | - | - | - |
| 1 | 364.32 | - | - | - | - |
| 2 | 559.90 | - | - | - | - |
| 3 | 439.64 | - | - | - | - |
| 4 | 293.84 | 26 | 42 | 1 | 1 |
| 5 | 376.16 | 14 | 40 | 5 | 11 |
| 6 | 158.52 | 11 | 41 | 1 | 3 |
| 7 | 222.98 | 15 | 44 | 1 | 3 |
| 8 | 354.47 | 12 | 48 | 3 | 2 |
| 9 | 584.00 | 10 | 109 | 6 | 8 |
| 10 | 230.14 | 18 | 58 | 3 | 4 |
| 11 | 306.84 | 31 | 156 | 3 | 5 |
| 12 | 79.69 | 21 | 46 | 1 | 3 |
| 13 | 646.07 | 17 | 67 | 3 | 4 |
| 14 | 209.32 | 22 | 41 | 1 | 0 |
| 15 | 105.44 | - | - | - | - |
| 16 | 489.97 | - | - | - | - |

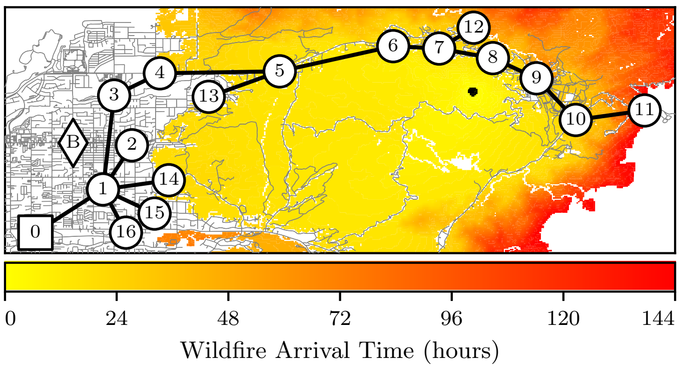


Fig. 1. The feeder (sections & switches), road network, and wildfire arrival time forecast for the case study. The square labeled 0 represents feeder section containing the substation. The circles labeled 1 through 16 represent feeder sections with load. The diamond labeled B is the utility's base of operations. The black area near section 8 represents the extent of the wildfire at the time the forecast is generated, and the gradient away from that area indicates the wildfire's forecasted time of arrival.

to more or less aggressively prioritize imminent decisions. For objective weights, which serve to normalize metrics with different magnitudes, units, and decision maker priorities, we select $\lambda^{\text{load}} = 1/\text{kW}$, $\lambda^{\text{job}} = 100$, and $\lambda^{\text{res}} = 10000$. These prioritize resource safety first, followed by load re-energization second, and job completion third.

### A. Distribution Feeder

Our case study incorporates a realistic but fictitious feeder defined on real geography. For this feeder, we select a subset of switches to comprise $\mathcal{L}$, from which the set of sections $\mathcal{N}$ follows. These switches and sections are depicted in Fig. 1. For each section $n$, we define criticality factor $\rho_n = 1$ and $p^{\text{load}}_{nt}$, assumed constant in time, as given in Table I. For section 0, which represents the substation, we define $p^{\text{supply}}_0 = 5421.30$ kW, the sum of all loads. For all other sections, $p^{\text{supply}}_n = 0$. We define $p^{\text{flow}}_{nm}$ to be arbitrarily large (*i.e.*, non-limiting) for all switches. The switch configuration set $\mathcal{O}$ we define as a singleton whose member corresponds to the directed tree rooted at section 0.

### B. Road Network

We obtain the road network in Fig. 1 from OpenStreetMap using the `osmnx` package for Python [5]. We define $\mathcal{S}$ as a set of 18 sites: one job site per section and one additional site representing the base of operations, the location of which we fabricated. Sites coincide with nodes in the road network. We fix many of the $z_{rst}$ variables to zero to ensure that resources start from the base of operations. Of the 306 possible (directed) site-to-site travel options, we restrict $\mathcal{Q}$ to just 34: the 17 from the base of operations to each section's site, and the 17 back. All site-to-site travel, when not prevented by the wildfire, requires less time than the duration of a single time period according to the OpenStreetMap data. We therefore set all site-to-site travel durations to one time period (*i.e.*, $d^{\text{travel}}_{s,s'} = 1$).

### C. Utility Response to Wildfire Impact

We suppose the utility's resources are a fleet of 20 crews, each providing a single 'repair' capability. We accordingly define $\mathcal{C} = \{\text{repair}\}$, $\mathcal{R} = \mathcal{R}_{\text{repair}} = \{\text{crew}\}$, and $a_{\text{crew}} = 20$.

To parametrize grid damage and restoration jobs, we select an arbitrary ignition point near the feeder and use FlamMap to simulate a wildfire for 144 hours. Based on the wildfire's simulated arrival time, which is shown in Fig. 1, and the locations of individual feeder components, we compute the parameters in the last four columns of Table I. The parameter $t^{\text{dmg}}_n$ is the time period the wildfire first reaches a component in the section, and $t^{\text{job}}_j$ is 12 time periods after the last component in the section intersects with the wildfire. The 12 time periods represent the delay between when the wildfire leaves the area and when the area becomes safe to enter. We suppose $t^{\text{job}}_j$ is uniform across all jobs in the same section. We estimate one transformer job per 4 transformers in the area of wildfire and one conductor job per 400 meters of conductor in the area of the wildfire. We suppose each transformer job requires 1 resource providing the 'repair' capability and 12 time periods to complete, and that each conductor job requires 3 resources providing the 'repair' capability and 16 time periods. Regarding the wildfire's impact on site and travel safety, for each job $j$ at site $s$ in section $n$ we suppose $\alpha_{st} = 1$ for all $t^{\text{dmg}}_n \leq t < t^{\text{job}}_j$. For each site-to-site travel option $(s, s')$ and time period $t$, we suppose $\beta_{ss't} = \max\{\alpha_{st}, \alpha_{s't}\}$. Otherwise, we suppose that sites and travel options are safe.

### D. Solution Methodology & Analysis of Results

We implemented the model using the `pyomo` package for Python [6], [7] and solved it directly using Gurobi [8] on an HP G5 Z6 workstation (AMD Ryzen Threadripper PRO 7975WX 32-Cores @ 4.00GHz, 160GB DDR4 RAM). We configured the solver to terminate after 60 seconds, at which point it returned a solution with a reported 1.79% MIP gap.

For the identified restoration schedule, Fig. 2 shows customer load served as a function of time. As expected, all sections with a conducting path to the substation, and only those sections, have their load served. Early in the time horizon, we observe a gradual decline in load served as the

979-8-3315-8138-1

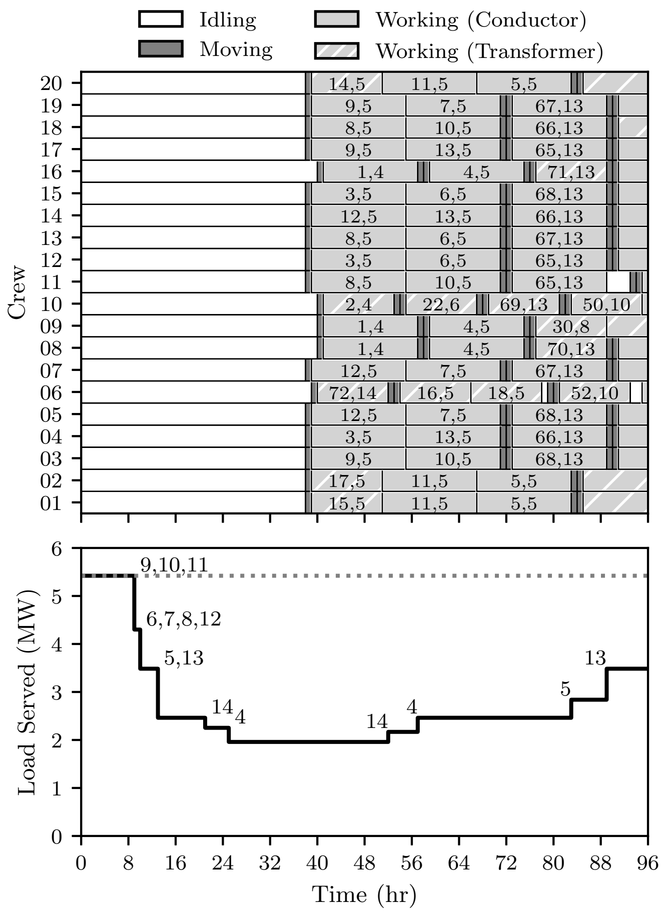


Fig. 2. The prescribed crew schedules (top) and served load (bottom) over the model time horizon. In the schedule plot, the unique job number and affected section are given for each working activity that completes within the finite time horizon. In the load plot, the numbers next to the falling and rising edges indicate the sections that are de- and re-energized, respectively.

wildfire damages sections, resulting in their de-energization. Later in the horizon, the solution prescribes the repair and re-energization of sections 14, 4, 5, and 13 in order. This restoration sequence aligns with our intuition regarding optimal strategy: repairs and re-energization occur in order of proximity to the substation as site and travel safety permit. In additional experiments involving more resources, we found that varying load criticality influenced the restoration order, with sections generally being re-energized in decreasing order of load criticality. This observation is consistent with our intuition about optimal restoration sequences and further validates the model.

The model solution describes how resources should be dispatched in aggregate based on type, but attaining a plan for individual resource use requires minimal postprocessing. In Fig. 2, we show a crew schedule derived from the identified solution. Indeed, all jobs in sections 14, 4, 5, and 13 are assigned crews. The solution features no conflicting assignments, no unnecessary travel, and just three occurrences of idle resources. These idle resources are presumably the suboptimalities contributing to the 1.79% MIP gap. As expected of an optimal resource dispatching plan, we observe high utilization of resources during the time when jobs are safe to complete.

## IV. Conclusion

We presented a co-optimization model designed to aid the restoration of wildfire-damaged electrical distribution systems. The results of our case study show that the model addresses the complexities of restoration decision making to optimize customer service, job scheduling, and resource safety. The case study, though simple, allowed us to validate the model by ensuring the identified solution aligns with our intuition.

We anticipate three directions for future work. First, we plan to incorporate job dependencies and inventory management for component replacements into the model. Second, we aim to expand the case study to further validate the model. Specifically, we seek to build a multi-feeder case study to exercise topology configuration and to define utility resources and jobs with more granularity (more resource types and capabilities, more heterogeneity in the job requirements, etc.). Additionally, we need to develop a simulation framework that facilitates using the model in a rolling-horizon approach and addressing forecast error. Third, we recognize that instances of our model involving many resource types, jobs, feeders, and other elements will be significantly larger and more challenging to solve than the case study presented. In particular, multiple switch configurations, which were not examined in this paper, could effect large discrete solution spaces. To efficiently solve our model at scale, we must improve our solution methodology, potentially through decomposition techniques that exploit the loose coupling of decisions across domains. These efforts will improve the model's effectiveness and trustworthiness for wildfire restoration and also broaden its applicability to other hazards, such as hurricanes, earthquakes, wind storms, etc.

## References


[1] "Bonneville Power Administration 2024 Wildfire Mitigation Plan," Portland, Oregon, 2024, available at: https://www.bpa.gov.

[2] C. Coffrin and P. Van Hentenryck, "Transmission system restoration with co-optimization of repairs, load pickups, and generation dispatch," *International Journal of Electrical Power & Energy Systems*, vol. 72, pp. 144–154, 2015, the Special Issue for 18th Power Systems Computation Conference. [Online]. Available: https://www.sciencedirect.com/science/article/pii/S0142061515001106

[3] A. Jalilian, B. Taheri, and D. K. Molzahn, "Co-optimization of damage assessment and restoration: A resilience-driven dynamic crew allocation for power distribution systems," *IEEE Transactions on Power Systems*, vol. 40, no. 1, pp. 676–688, 2025.

[4] M. Finney, S. Brittain, R. C. Seli, C. McHugh, and L. Gangi, "Flammap: Fire mapping and analysis system (version 6.2)," Software, 2023, available at: https://www.firelab.org/project/flammap.

[5] G. Boeing, "Modeling and analyzing urban networks and amenities with osmnx," *Geographical Analysis*, vol. 57, no. 4, pp. 567–577, 2025. [Online]. Available: https://onlinelibrary.wiley.com/doi/abs/10.1111/gean.70009

[6] W. E. Hart, J.-P. Watson, and D. L. Woodruff, "Pyomo: modeling and solving mathematical programs in python," *Mathematical Programming Computation*, vol. 3, no. 3, pp. 219–260, 2011.

[7] M. L. Bynum, G. A. Hackebeil, W. E. Hart, C. D. Laird, B. L. Nicholson, J. D. Siirola, J.-P. Watson, and D. L. Woodruff, *Pyomo–optimization modeling in python*, 3rd ed. Springer Science & Business Media, 2021, vol. 67.

[8] Gurobi Optimization, LLC, "Gurobi Optimizer Reference Manual," 2025, available at https://www.gurobi.com.


979-8-3315-8138-1